Topology of Induced Lunar Magnetic Fields

K. Schwartz

20858 Collins Street
Woodland Hills, California
91364

and

G. Schubert

Department of Planetary and Space Science
University of California, Los Angeles
90024

PREPARED UNDER CONTRACT NAS 2-6876

Abstract

Using the asymmetric theory of lunar induction derived by Schubert et al. (1973a), we have obtained the total and induced magnetic field line structure within the Moon and the diamagnetic cavity. Total field distributions are shown for orientations of the oscillating interplanetary field parallel, perpendicular and at 45° to the cavity axis. Induced field lines are shown only for the orientations of the interplanetary field parallel and orthogonal to the cavity axis. When compared with the field lines derived using the long wavelength limit of spherically symmetric vacuum induction theory, the configurations obtained using the asymmetric theory exhibit significant distortion. For all orientations of the interplanetary field, the field lines are strongly compressed on the sunlit hemisphere because of the confining solar wind pressure at the lunar surface and the exclusion of the field by the lunar "core". Field line compression is also observed in the antisolar region in agreement with the experimental observations of Schubert et al. (1973b) and Smith et al. (1973). For the parallel orientation of the interplanetary field, antisolar compression is caused by cavity confinement of the induced field. For the interplanetary field perpendicular to the cavity axis there is, in addition to compression by the cavity boundary, redistribution of field lines from the sunlit to the night side. In this case field lines

entering the Moon just forward of the limb pass through the lunar "crust" on the night side and then exit forward of the limb. This phenomenon manifests itself as a displacement of the null in the induced magnetic field at the surface sunward of the limb, in striking similarity to the magnetospheric field lines of the Earth.

1. Introduction

Schubert et al. (1973a) have derived an analytic solution for the magnetic field within a spherical Moon and its downstream cylindrical cavity formed by the solar wind for time dependent interplanetary magnetic fields both parallel and perpendicular to the cavity axis. By superposition, the solution is known for arbitrary orientations of the interplanetary field. The theory is quasistatic (low frequency) and is formulated in terms of a scalar magnetic potential. Thus the Moon model consists of a perfectly conducting core of radius b surrounded by a nonconducting shell of thickness a-b (a is thus the lunar radius); the cavity has radius a, extends infinitely far downstream and is also nonconducting. Outside the Moon and its diamagnetic cavity the magnetic field is everywhere the given interplanetary field. The frequency of the interplanetary magnetic field oscillations appears implicitly in the quasistatic model through the radius of the infinitely conducting core which limits the depth of penetration of electromagnetic waves. The theory has been used successfully by Smith et al. (1973) to interpret the frequency dependence and lunar longitude variations of the Apollo 12 lunar surface magnetometer data.

In this paper we use the asymmetric theory of Schubert et al. (1973a) to provide a picture of both the total and induced magnetic field line distributions in and around the Moon for certain orientations of the interplanetary field fluctuations. These field line

pictures are compared with the distributions one would obtain using a spherically symmetric vacuum theory of lunar induction. We find that the induced lunar field line distribution bears a marked resemblance to the structure of the solar wind distorted geomagnetic field.

The magnetic field line distributions were obtained by numerically integrating the differential equations

$$\frac{dx}{B_x} = \frac{dy}{B_y} = \frac{dz}{B_z}$$

where (dx, dy, dz) are the Cartesian components of a field line element. The spatial dependence of the magnetic field components B_x , B_y and B_z is given by Schubert et al. (1973a) for the asymmetric theory. They also provide the dependence of B_x , B_y B_z on (x,y,z) for the symmetric vacuum theory (this theory is considered here by way of comparison to the distorted asymmetric field lines and also to provide a check on the computer program since the symmetric vacuum field line distribution is known analytically).

Following Schubert et al. (1973a) we have carried out the calculations for the interplanetary field either parallel, perpendicular, or at 45° to the axis of the diamagnetic cavity. For the latter case only the total field is shown. When the inter-

planetary field is parallel to the cavity axis we have calculated the field lines in a plane which passes through the cavity axis. Because of symmetry this plane can make any angle with the ecliptic. For the cases in which the interplanetary field is either perpendicular or at 45° to the cavity axis, we have calculated the field lines in the plane containing the cavity axis and the interplanetary field. If the interplanetary field is either parallel or perpendicular to the cavity axis we show the field line configurations derived from both the asymmetric theory and the symmetric vacuum theory. For ease of direct comparison, the two sets of field lines are drawn on the same figure on opposite sides of the lunar diameter and cavity axis..

Finally we note that the field lines represent the instantaneous spatial distribution of the magnetic field for a harmonic excitation of the form $e^{-i\omega t}$ where ω is the angular frequency. The theory itself does not contain the frequency explicitly; it appears implicitly in the choice of the ratio b/a. For low frequencies the appropriate b/a is small, while for high frequencies it approaches unity (Smith et al., 1973).

2. Distribution of the Total Magnetic Field

Figures 1-4 show the distributions of the total magnetic field for the interplanetary field parallel to the cavity axis and for $b/a = 0.6, 0.7, 0.8$ and 0.9, respectively. Each figure is divided by the cavity axis and lunar diameter into two parts; the upper part showing the asymmetric field lines and the lower part the spherically symmetric vacuum (SSV) field lines. The calculations were started sufficiently far upstream of the Moon that the field lines were originally parallel to each other and equally spaced. The numerical identification of the field lines corresponds to the distance in lunar radii, o/a, of the undistorted interplanetary field lines from the cavity axis. The negative numbers go with the SSV lines.

In the asymmetric portion the field lines outside the Moon and the cavity are all equally spaced since the low frequency induced field cannot propagate upstream in the solar wind and downstream propagation is limited to the interior of the conical surface tangent to the lunar limb and making the Mach angle with the downstream direction. Since the Mach angle is small the conical surface can be approximated by the cylindrical surface of the cavity. Inside the Moon, field lines are strongly compressed between the lunar surface and the core. This field compression increases from its value at the subsolar point to a maximum at

the terminator, whereupon it decreases with proximity to the antisolar point. This decrease in the field line compression results from the expansion of field lines into the cavity. However, compressive effects are still visible at the lunar surface even at the antisolar point because of the confinement of the field by the cavity walls. This is contrasted with the field line distribution obtained using SSV theory. The SSV lines begin to "see" the Moon well upstream of the lunar surface and also for $\rho/a > 1$. Further,interplanetary lines which would intercept the lunar disk in the asymmetric theory are able to bend out far beyond the lunar limb in the SSV case.

The asymmetric distortion of the field lines is seen to be more pronounced for larger b/a, i.e. for interplanetary fields of higher frequency which damp at shallow depths in the Moon. The relative maxima in the radial field components at the lunar surface near the limb, shown in Figure 2 of Schubert et al. (1973a) for b/a = 0.8 and 0.9, are easily visualized in terms of the increased density of field lines threading the lunar surface just downstream of the limb. Finally the field line configuration for the spherically symmetric confined theory (SSP) (also discussed in Schubert et al. (1973a)) is identical to that of the asymmetric case on the lunar sunlit side.

The field line configurations for the case of the driving

field orthogonal to the cavity axis are shown in Figures 5-8 for the same values of b/a as before. The asymmetric field lines are shown to the left of the cavity axis and the SSV lines to the right. The lines are identified by the distance, in lunar radii, of the undisturbed field line from the lunar diameter connecting the limbs. The field lines of the asymmetric theory exhibit strong compression on the sunward side and a lesser degree of compression on the dark side. The strong day-night asymmetry is clearly in evidence as contrasted with the day-night symmetry of the SSV distribution. For the cases b/a = 0.8 and 0.9 (Figures 7 and 8) the asymmetric field lines marked -0.1 close within the Moon but on the dark side. There is a redistribution of field lines from the lunar sunlit side to the lunar night side which is qualitatively similar to the "peeling back" of field lines in the Earth's magnetosphere. This effect of redistribution increases in importance with increasing b/a and corresponds to the shifting of the null in the surface tangential magnetic field forward of the limb, i.e. toward the Sun. This "flipping" of a field line from the front to the back adds to the tangential field compression on the dark side. It also accounts for the difference between the front side tangential fields calculated by the asymmetric theory and by SSP theory. As reported by Schubert et al. (1973a), this difference increases with increasing b/a, SSP theory giving the larger tangential sunlit side field. For b/a = 0.6 and 0.7 the -0.1 field line is on the sunlit

side, however, there is still some redistribution. The asymmetric distributions on the dark side suggest a decrease in the radial component of the surface magnetic field. Except near the limb this is indeed the case. In fact for b/a = 0.9 Schubert et al. (1973a) reported almost no radial field for angles up to 60° from the antisolar point.

It was pointed out by Schubert et al. (1973a) that the response of the Moon to an interplanetary field making an arbitrary angle with the cavity axis could be synthesized by properly combining responses derived from the two cases discussed above. In Figures 9-12 we show the asymmetric field lines when the interplanetary field makes an angle of 45° with the cavity axis. As noted previously, there is no effect on the interplanetary field upstream of the Moon or outside of the cavity. There is strong compression of the tangential fields on the sunward side and even beyond the limb or the dark side. The field line redistribution can be observed for b/a = 0.8 and 0.9. The effect of the Moon on the field in the cavity extends from one to two lunar radii downstream of the limb and then falls below the level where it can be seen in the figures.

3. Distribution of the Induced Magnetic Field

To more clearly examine the differences between the SSV and asymmetric theories we have obtained the induced field line distributions. The field lines induced by an interplanetary field parallel to the cavity axis are shown in Figures 13-16 for the same b/a values as considered in earlier figures. The contrast between the results of the SSV and asymmetric theories is enhanced when only the induced fields are compared. The day-night asymmetry stands out clearly and the asymmetric field lines take on the appearance of being "blown back" by the containment effect of the solar wind in contrast to the symmetric field lines of the SSV theory. The front side compression is also clearly visible as is the compression at and beyond the limb. The rapid decrease of the asymmetric field with distance down the cavity is also vividly shown, even for b/a = 0.9, as compared with the far reaching field configuration of the SSV theory.

The induced field lines for the case of the interplanetary field perpendicular to the cavity axis are shown in Figures 17-20 for the different values of b/a. The asymmetric lines are again in sharp contrast with the SSV field lines. Field line redistribution is seen even for b/a = 0.6 with the accompanying displacement of the null in the surface tangential field toward the Sun. This configuration shows a striking similarity to the

field line distribution of the Earth's dipolar field as distorted by the solar wind. Because of the low back pressure of the lunar induced field we see that the sunward surface of the Moon plays the role of the Earth's magnetopause, but the general features of the two configurations are very similar with the lunar magnetic field lines originating sunward of the dipole axis being blown far back into the lunar cavity.

4. Remarks

The magnetic field line distributions presented in this paper are representative of the lunar induced fields at the low frequencies for which the theory of Schubert et al. (1973a) is a proper description of the interaction of the interplanetary field with the Moon. The frequencies for which this theory is a valid approximation generally lie below about 0.01 Hz. This follows from the good agreement between theory and observation reported by Smith et al. (1973). In addition Schubert and Schwartz (1972) have shown that in the SSP theory, high frequency effects could be ignored for $2\pi a/\lambda \lesssim 1/4$, where λ is the wavelength of the interplanetary field fluctuation. For a wave velocity of 4×10^5 m/s this criterion corresponds to a frequency of about 0.01 Hz. This is the speed one might expect for waves propagating outward from the Sun. For waves propagating transverse to the cavity axis a slightly smaller speed may be likely and thus the quasistatic asymmetric theory would be valid for somewhat smaller frequencies.

References

Schubert, G. and Schwartz, K.: 1972, 'High Frequency Electromagnetic Response of the Moon,' J. Geophys. Res. 77, 76.

Schubert, G., Sonett, C.P., Schwartz, K., and Lee, H.J.: 1973a, 'The Induced Magnetosphere of the Moon I. Theory,' submitted to J. Geophys. Res.

Schubert, G., Smith, B.F., Sonett, C.P., Colburn, D.S., and Schwartz, K.: 1973b, 'The Night Side Electromagnetic Response of the Moon,' submitted to J. Geophys. Res.

Smith, B.F., Colburn, D.S., Schubert, G., Schwartz, K., and Sonett, C.P.: 1973, 'The Induced Magnetosphere of the Moon II. Experimental Results from Apollo 12 and Explorer 35,' in preparation.

Figure Captions

Figure 1. Field line configuration for the total magnetic field with the interplanetary field parallel to the cavity axis and b/a = 0.6. The field lines in the upper half of the figure were derived using the asymmetric theory of lunar induction. The lower half of the figure was obtained using the long wavelength limit of spherically symmetric vacuum (SSV) induction theory. The core radius corresponds roughly to the frequency of the interplanetary field with higher frequencies corresponding to larger values of b/a. Note the compression of the asymmetric lines in contrast to the SSV theory.

Figure 2. Same as Figure 1 with b/a = 0.7.

Figure 3. Same as Figure 1 with b/a = 0.8.

Figure 4. Same as Figure 1 with b/a = 0.9.

Figure 5. Field line configuration for the total magnetic field with the interplanetary field perpendicular to the cavity axis and b/a = 0.6. The field lines in the left half of the figure correspond to the asymmetric theory while those on the right correspond to the SSV theory.

Figure 6. Same as Figure 5 except b/a = 0.7.

Figure 7. Same as Figure 5 except b/a = 0.8. Note that in addition to field line compression there is also a redistribution of field lines in the asymmetric case. Field lines entering the lunar surface sunward of the limb pass through the lunar crust and exit on the dark side.

Figure 8. Same as Figure 7 except b/a = 0.9.

Figure 9. Field line configuration for the total magnetic field based on asymmetric theory with an oscillatory interplanetary field at 45° to the cavity axis (b/a = 0.6).

Figure 10. Same as Figure 9 but with b/a = 0.7.

Figure 11. Same as Figure 9 but with b/a = 0.8.

Figure 12. Same as Figure 9 but with b/a = 0.9.

Figure 13. Field line configuration of the induced magnetic field with the interplanetary field parallel to the cavity axis and b/a = 0.6. The right half of the figure corresponds to the asymmetric theory while the left corresponds to SSV theory. Note

Figure 13 (continued)

the strong front side and cavity compression with the appearance of "swept back" field lines for the asymmetric case.

Figure 14. Same as Figure 13 but with b/a = 0.7.

Figure 15. Same as Figure 13 but with b/a = 0.8.

Figure 16. Same as Figure 13 but with b/a = 0.9.

Figure 17. Field line configuration for the induced magnetic field with the interplanetary field perpendicular to the cavity axis and b/a = 0.6. The left half of the figure corresponds to the asymmetric theory, the right half to SSV theory. The asymmetric configuration exhibits the compression by the solar wind and cavity walls, the "peeling back" of field lines causing them to close behind the Moon instead of in front and the accompanying displacement of the null point on the surface sunward of the limb.

Figure 18. Same as Figure 17 except b/a = 0.7.

Figure 19. Same as Figure 17 except b/a = 0.8.

Figure 20. Same as Figure 17 except b/a = 0.9.

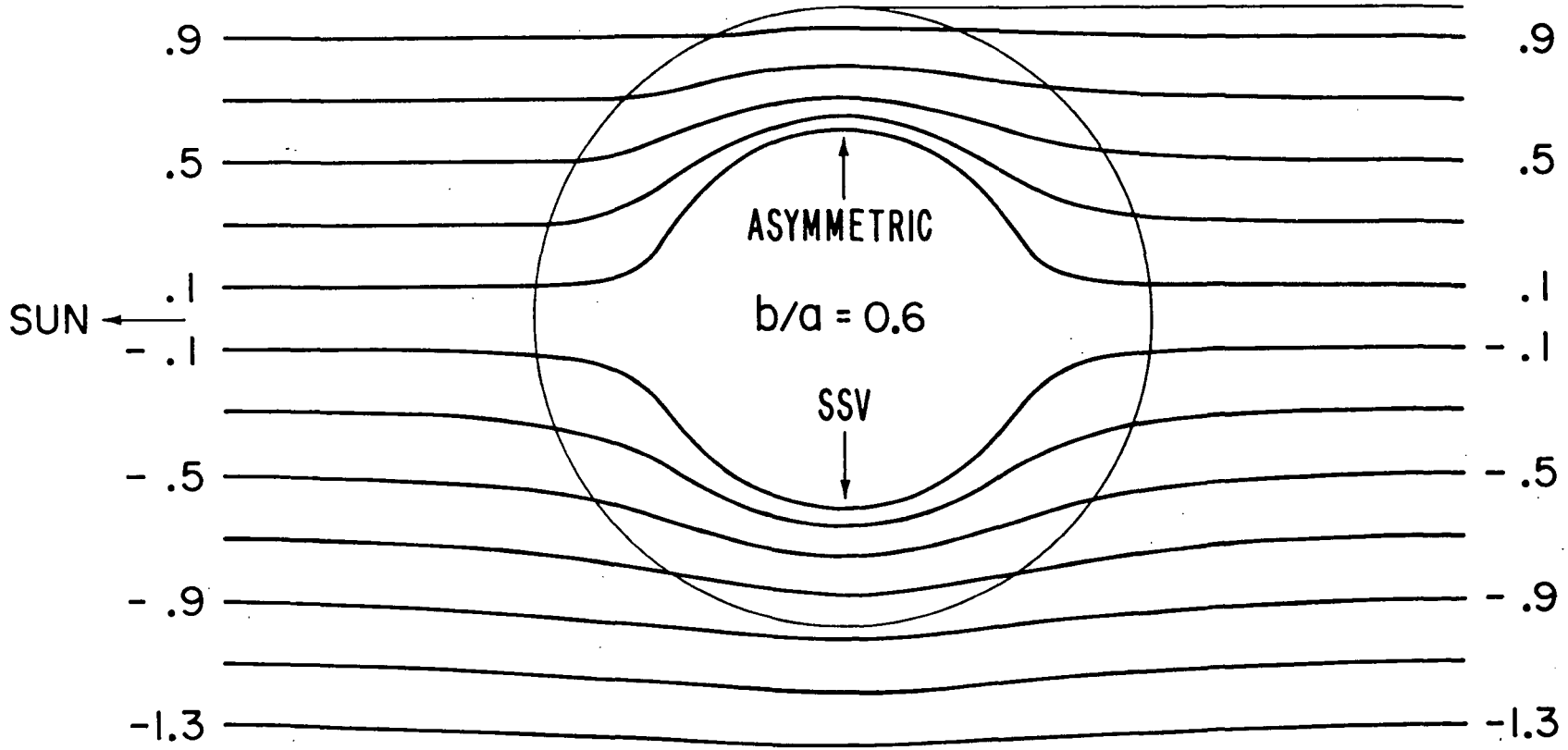
.9
.5
.1
SUN
- .1
- .5
- .9
-1.3
ASYMMETRIC
b/a = 0.6
SSV
.9
.5
.1
- .1
- .5
- .9
-1.3

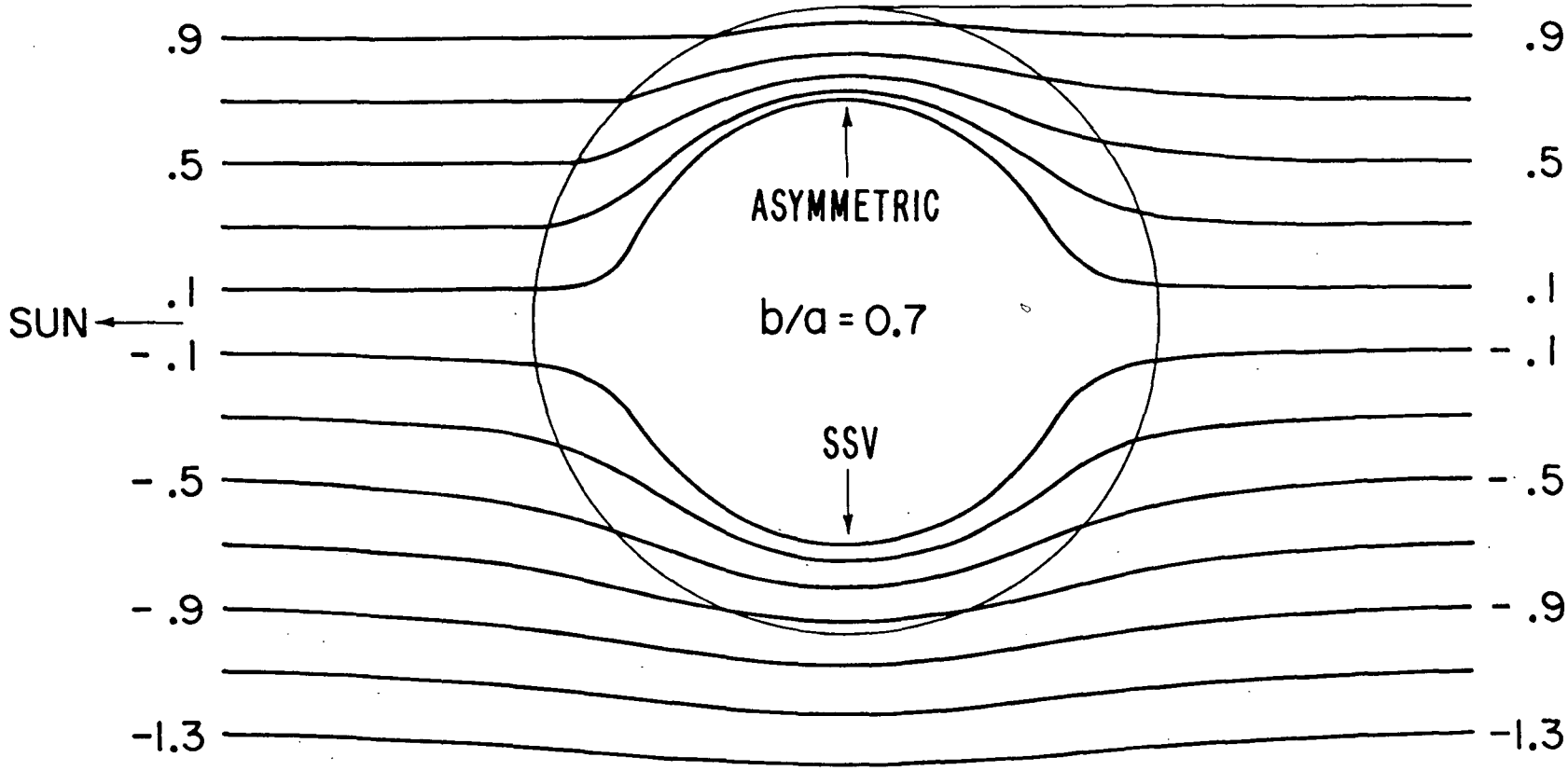
.9
.5
.1
SUN
- .1
- .5
- .9
-1.3
ASYMMETRIC
b/a = 0.7
SSV
.9
.5
.1
- .1
- .5
- .9
-1.3

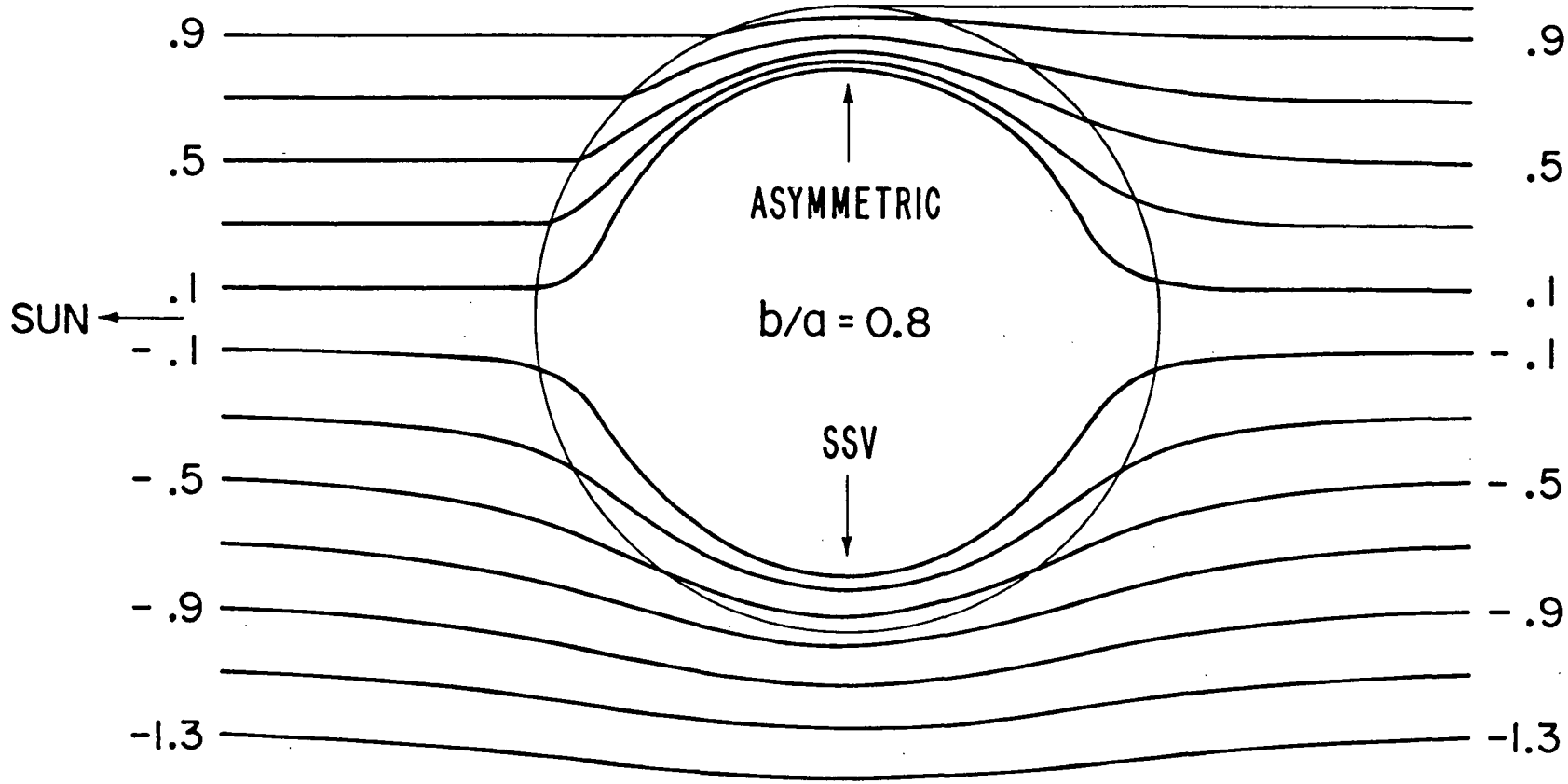
.9
.5
.1
SUN
- .1
- .5
- .9
-1.3
ASYMMETRIC
b/a = 0.8
SSV
.9
.5
.1
- .1
- .5
- .9
-1.3

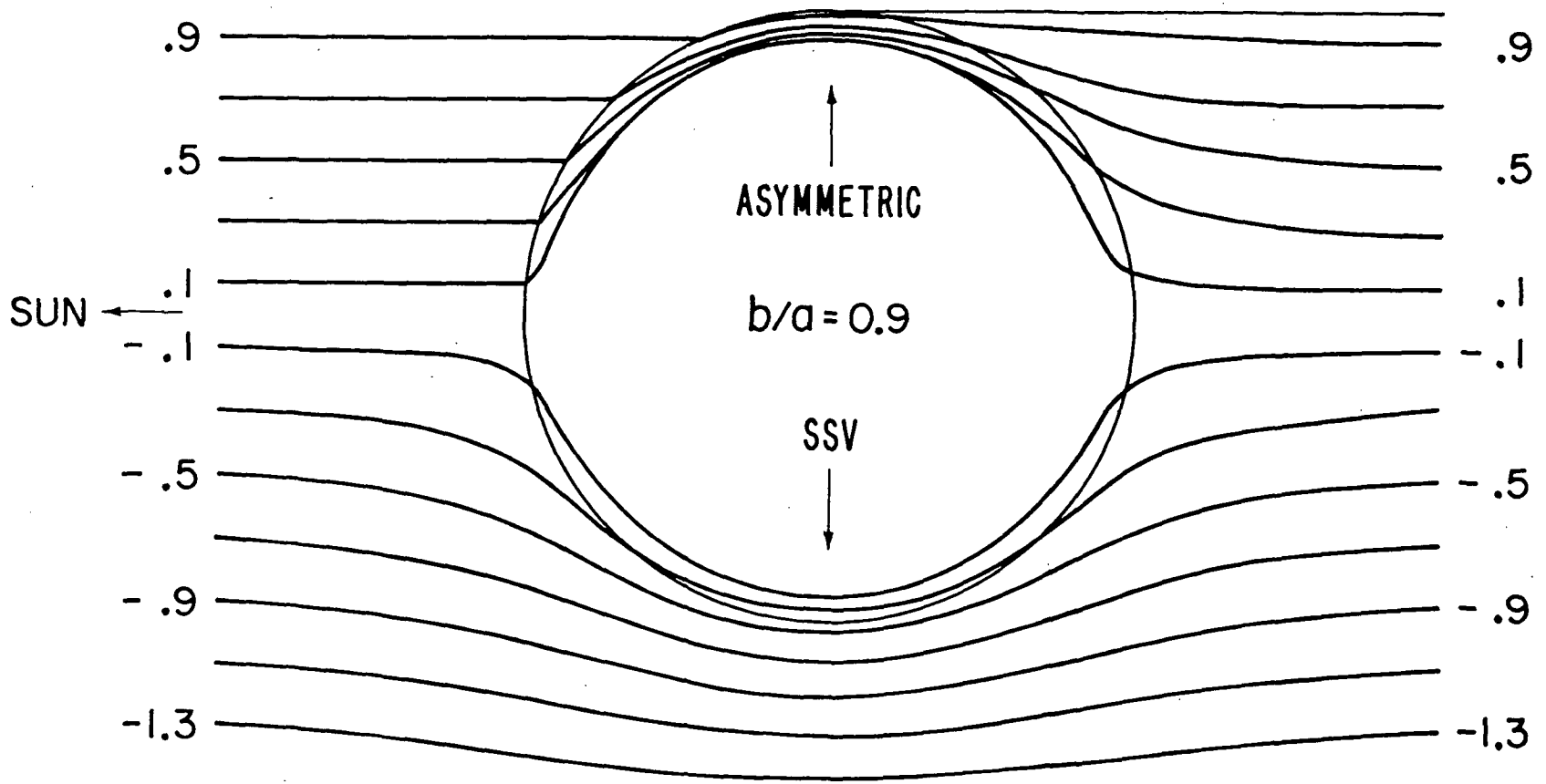
.9
.5
.1
SUN
-.1
-.5
-.9
-1.3
ASYMMETRIC
b/a = 0.9
SSV
.9
.5
.1
-.1
-.5
-.9
-1.3

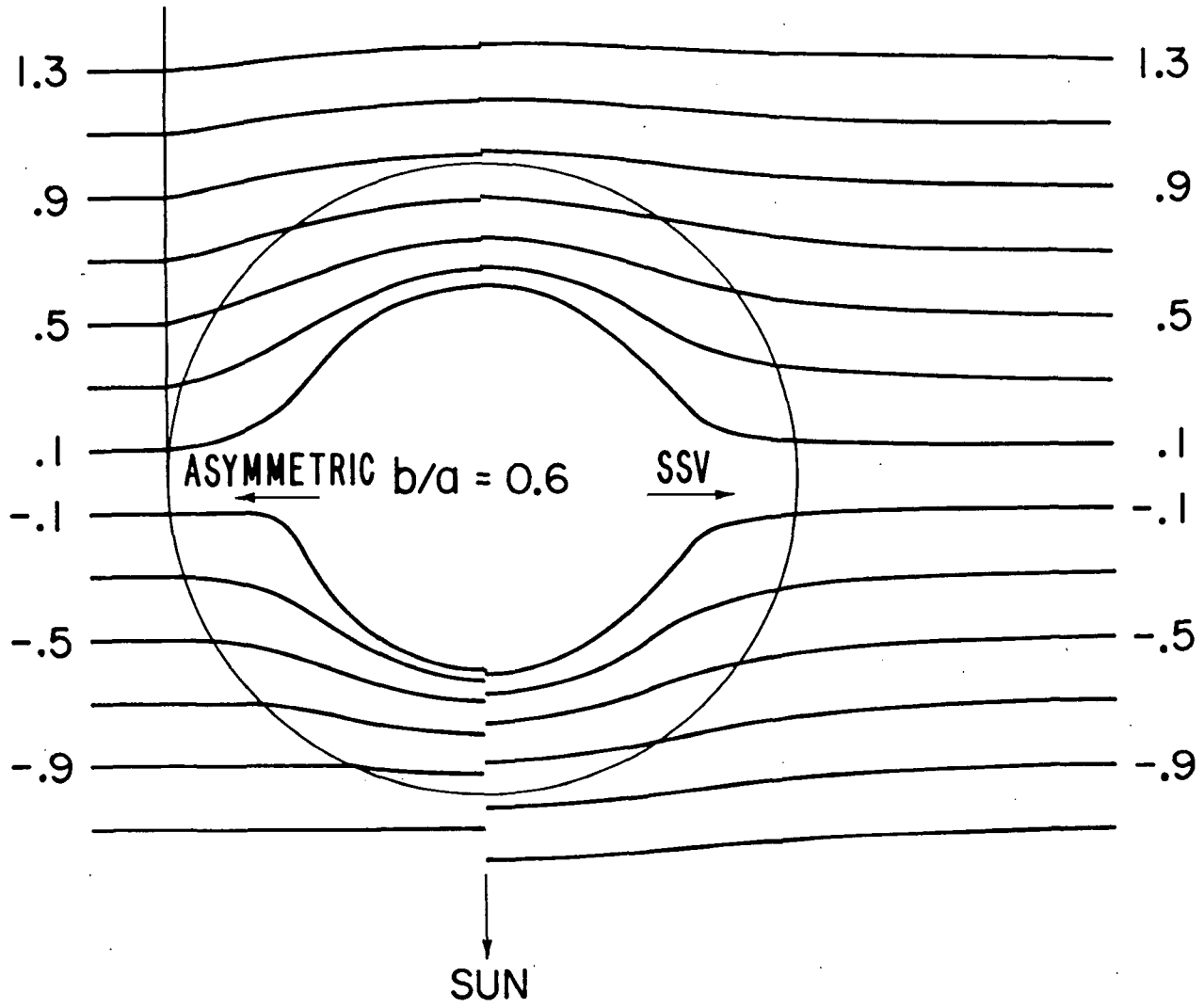
1.3
.9
.5
.1
-.1
-.5
-.9
1.3
.9
.5
.1
-.1
-.5
-.9
ASYMMETRIC b/a = 0.6
SSV
SUN

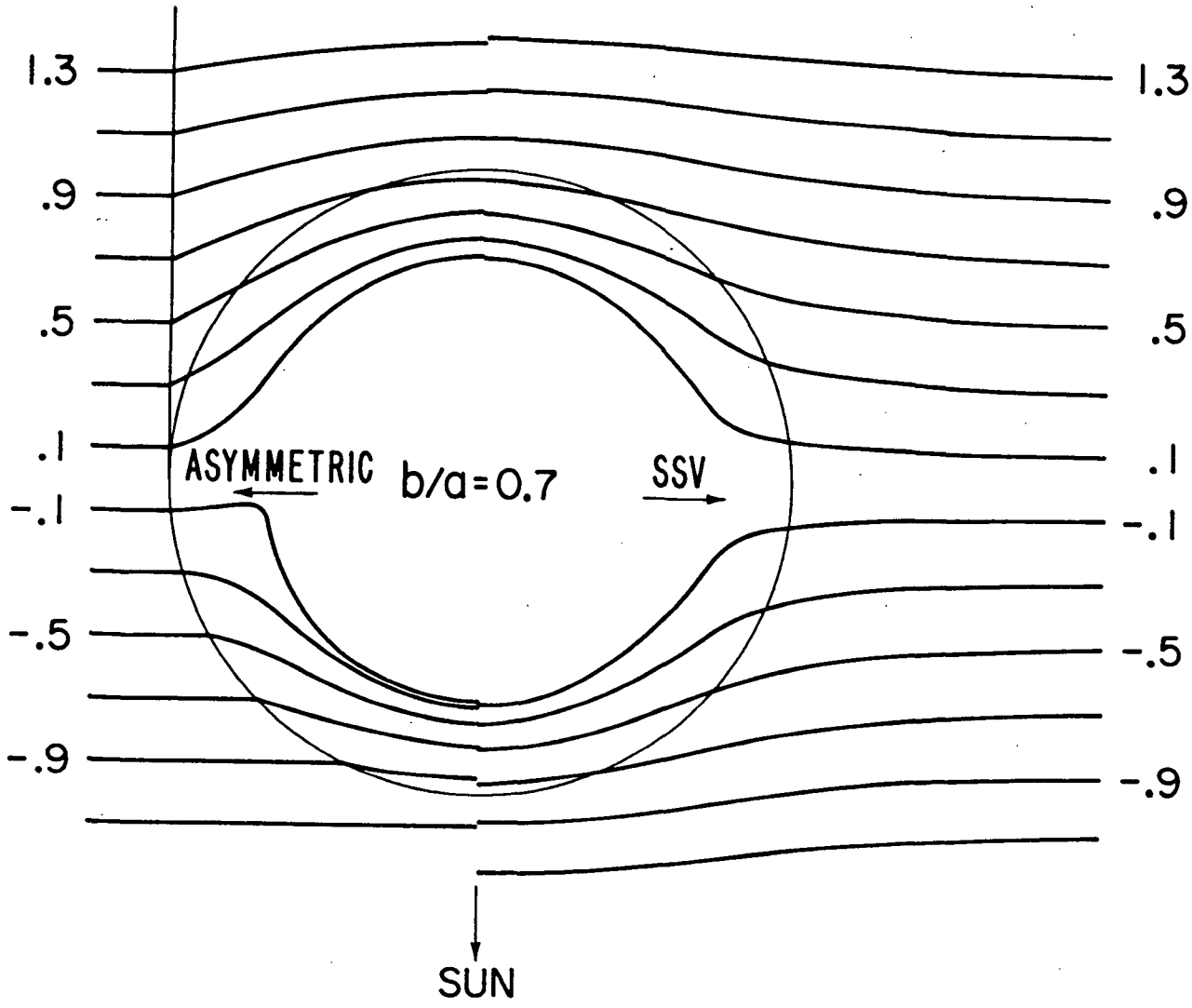
1.3
.9
.5
.1
-.1
-.5
-.9
1.3
.9
.5
.1
-.1
-.5
-.9
ASYMMETRIC
b/a=0.7
SSV
SUN

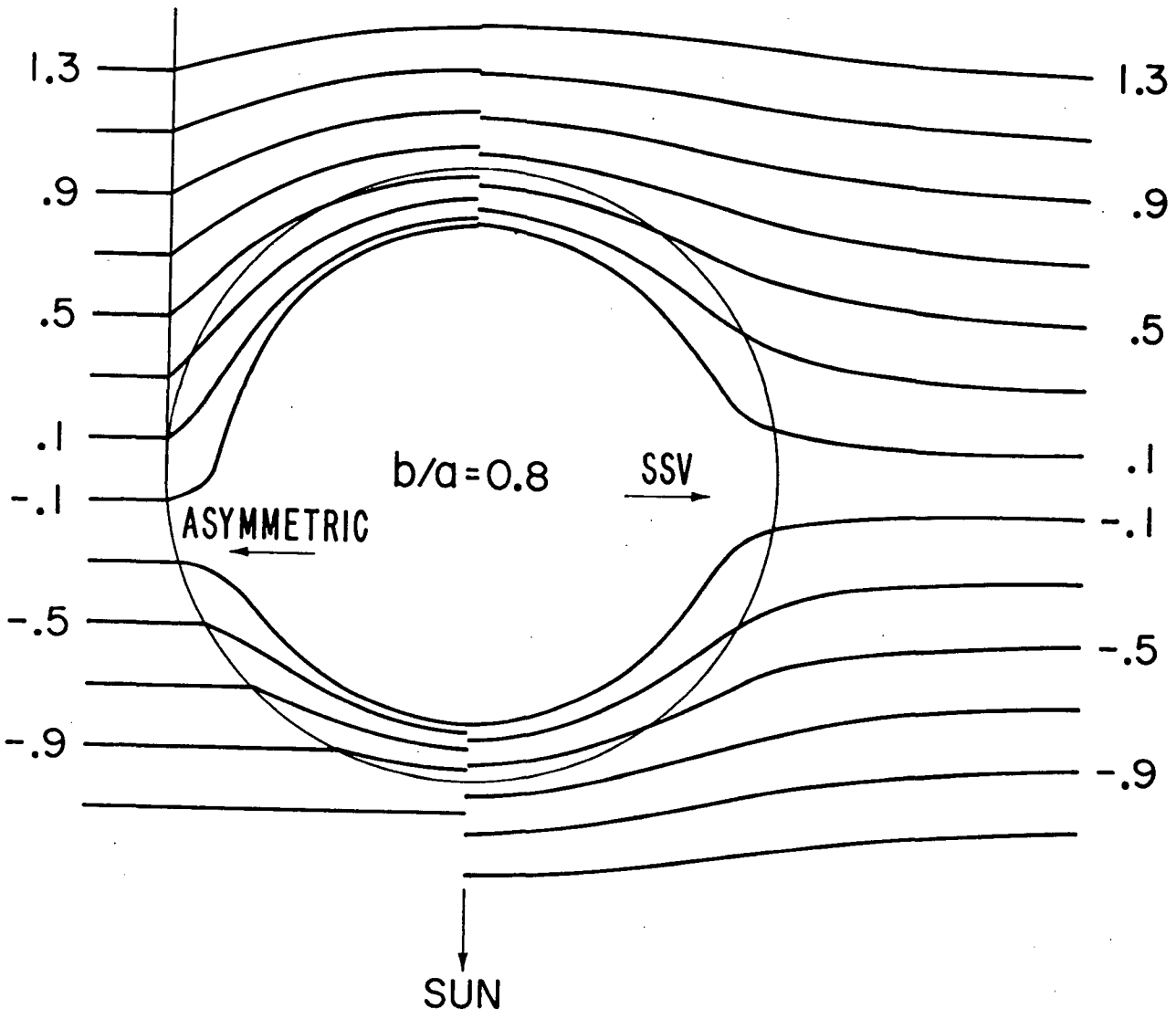
1.3
.9
.5
.1
-.1
-.5
-.9
1.3
.9
.5
.1
-.1
-.5
-.9
b/a=0.8
SSV
ASYMMETRIC
SUN

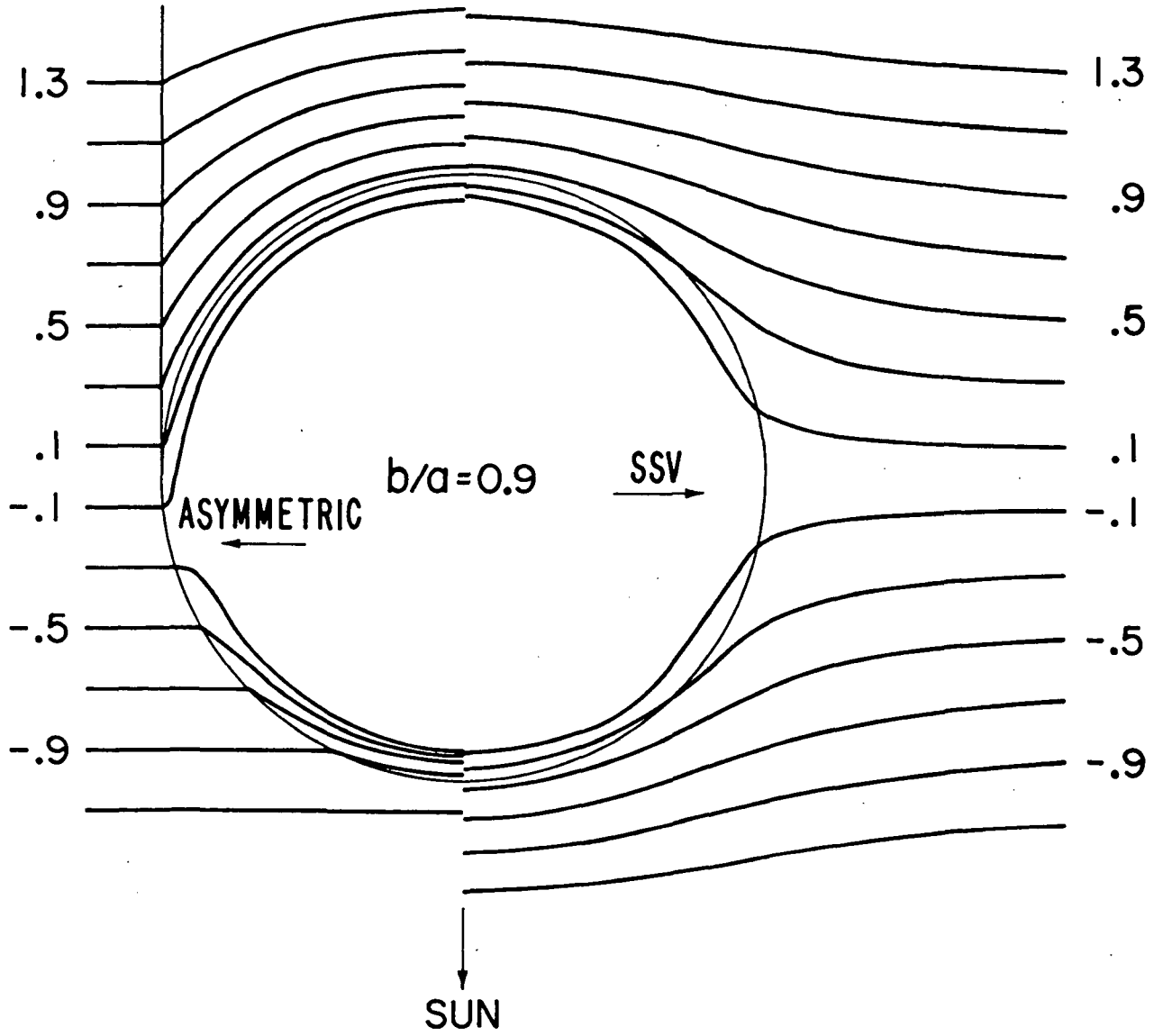
1.3
.9
.5
.1
-.1
-.5
-.9
1.3
.9
.5
.1
-.1
-.5
-.9
ASYMMETRIC
b/a=0.9
SSV
SUN

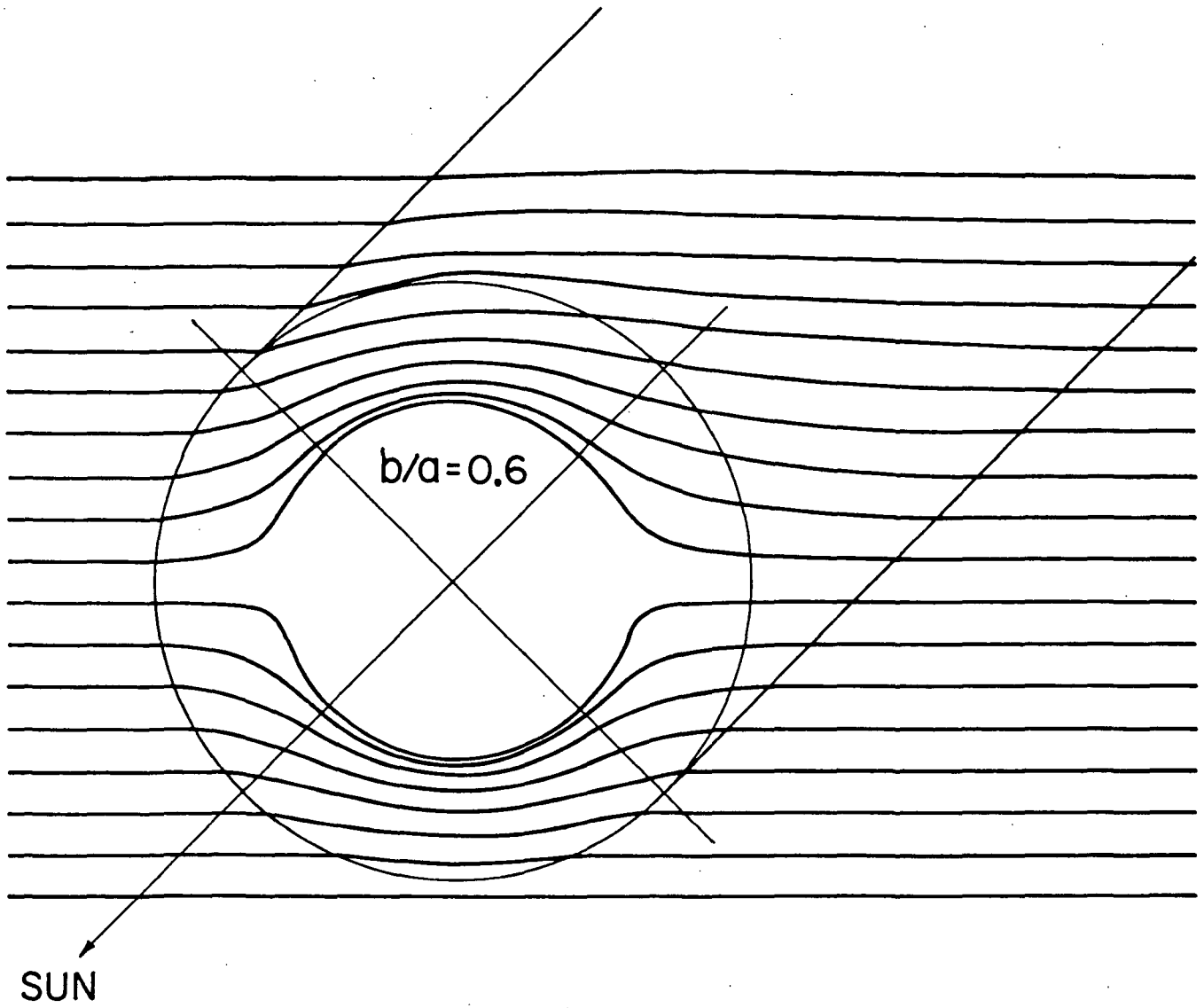
b/a=0.6
SUN

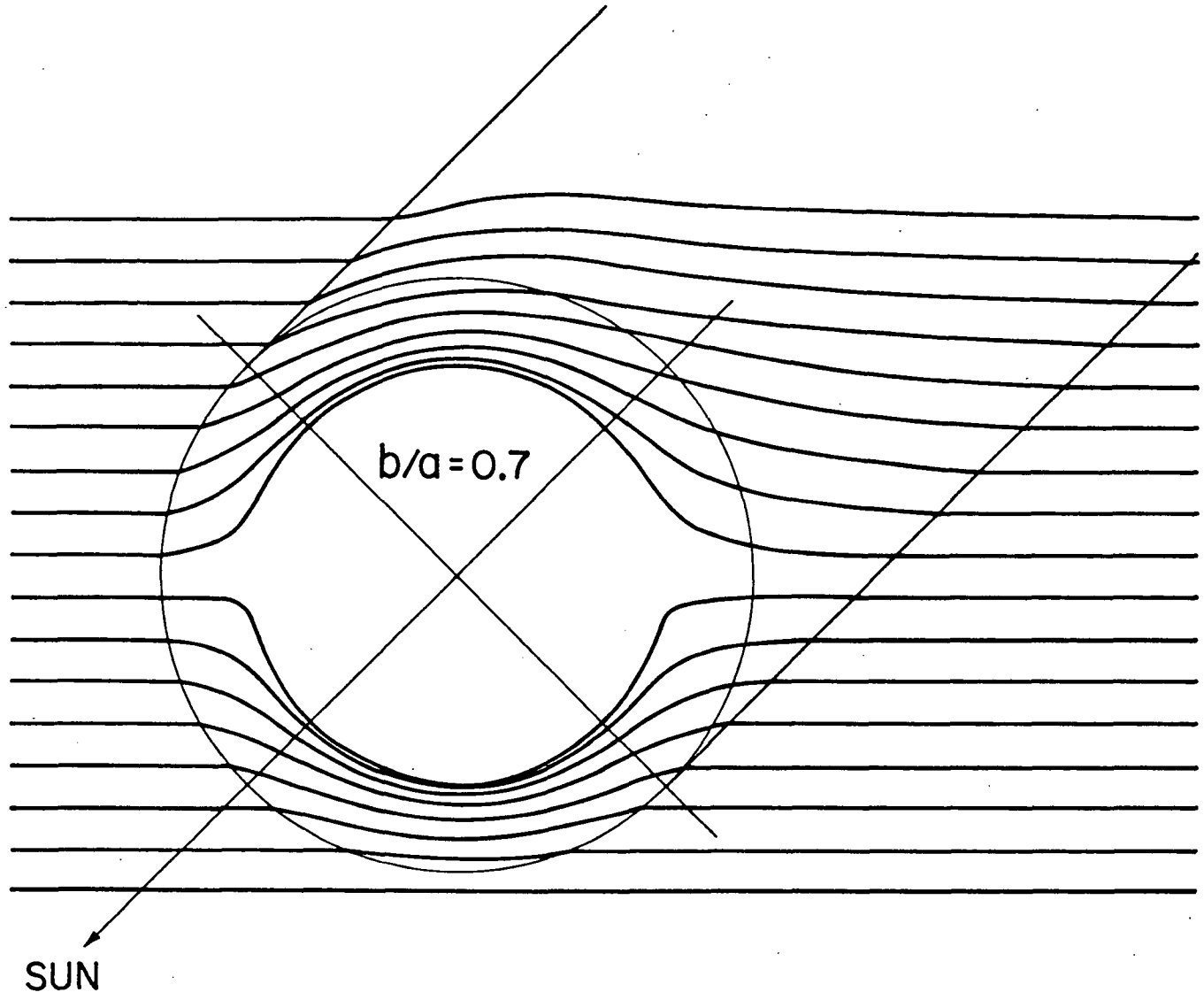
b/a = 0.7
SUN

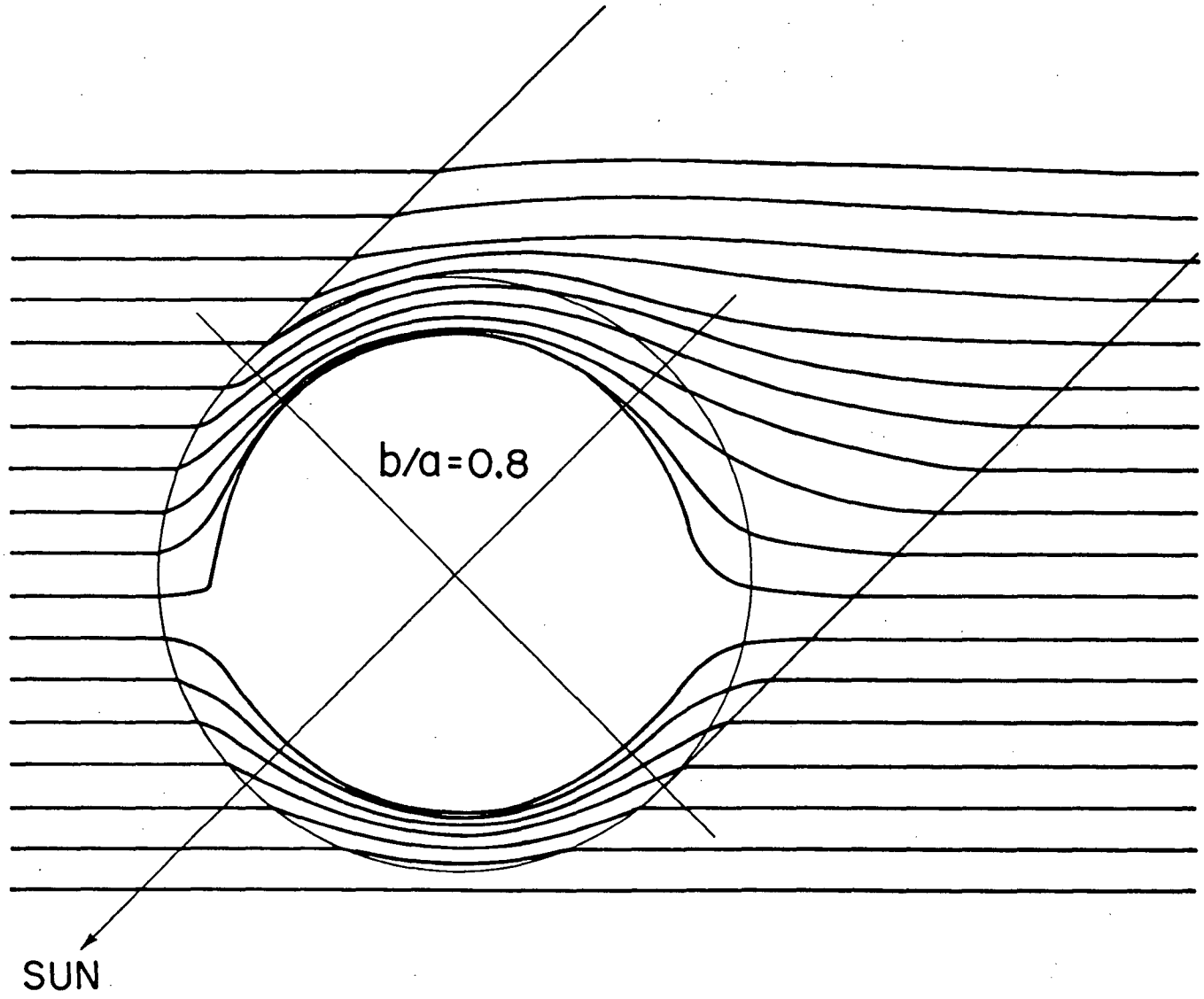
b/a=0.8
SUN

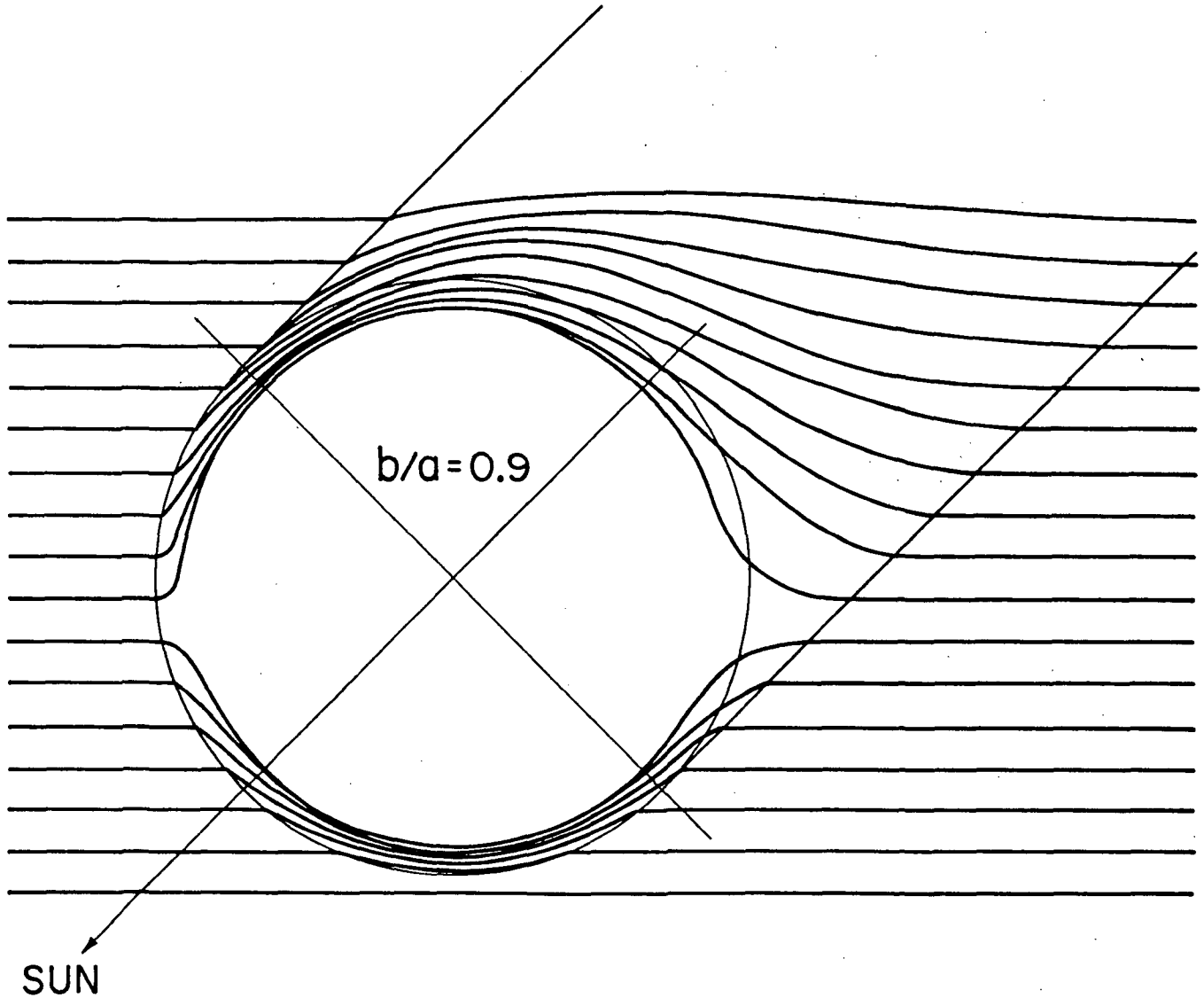
b/a=0.9
SUN

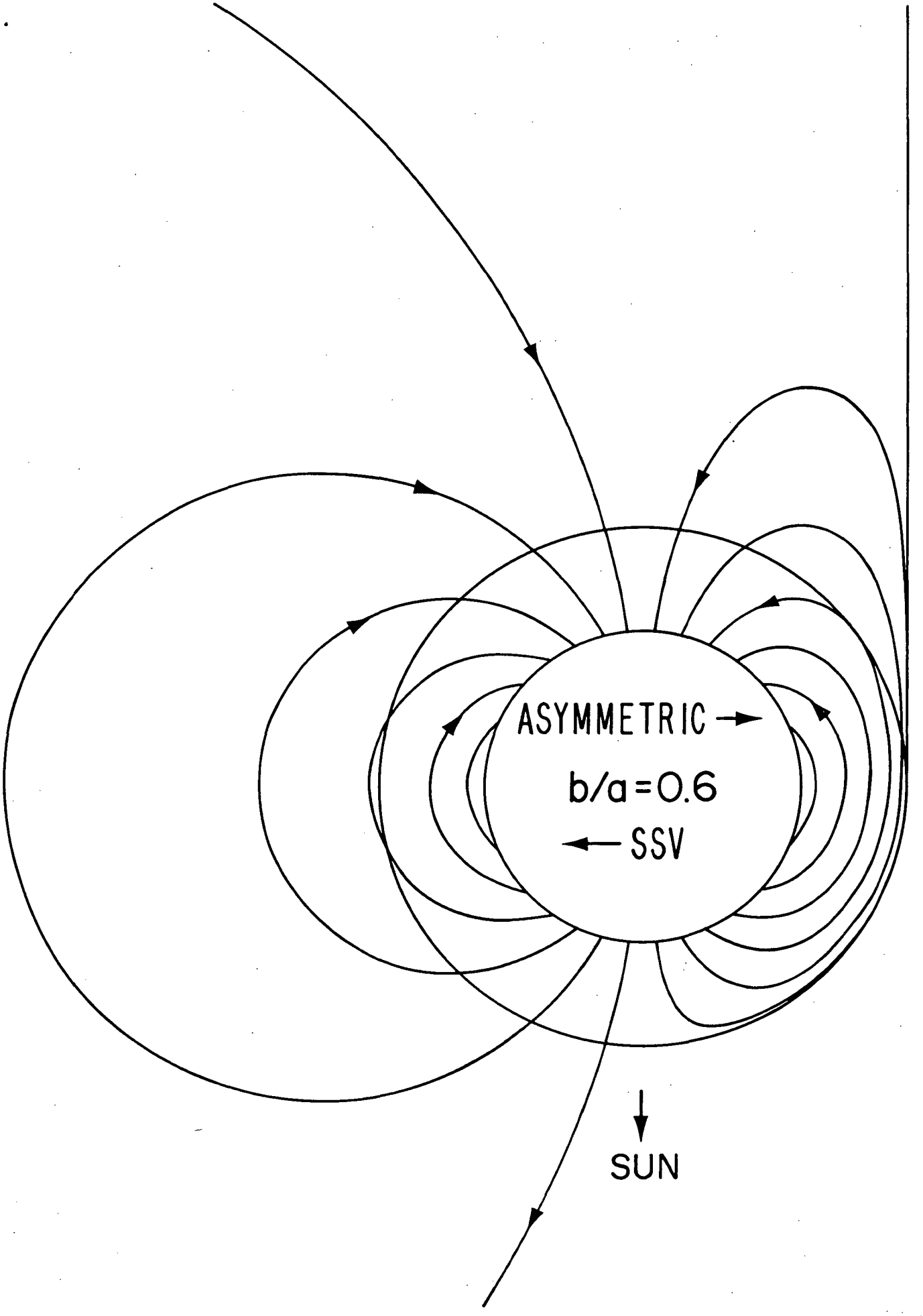
ASYMMETRIC
b/a=0.6
SSV
SUN

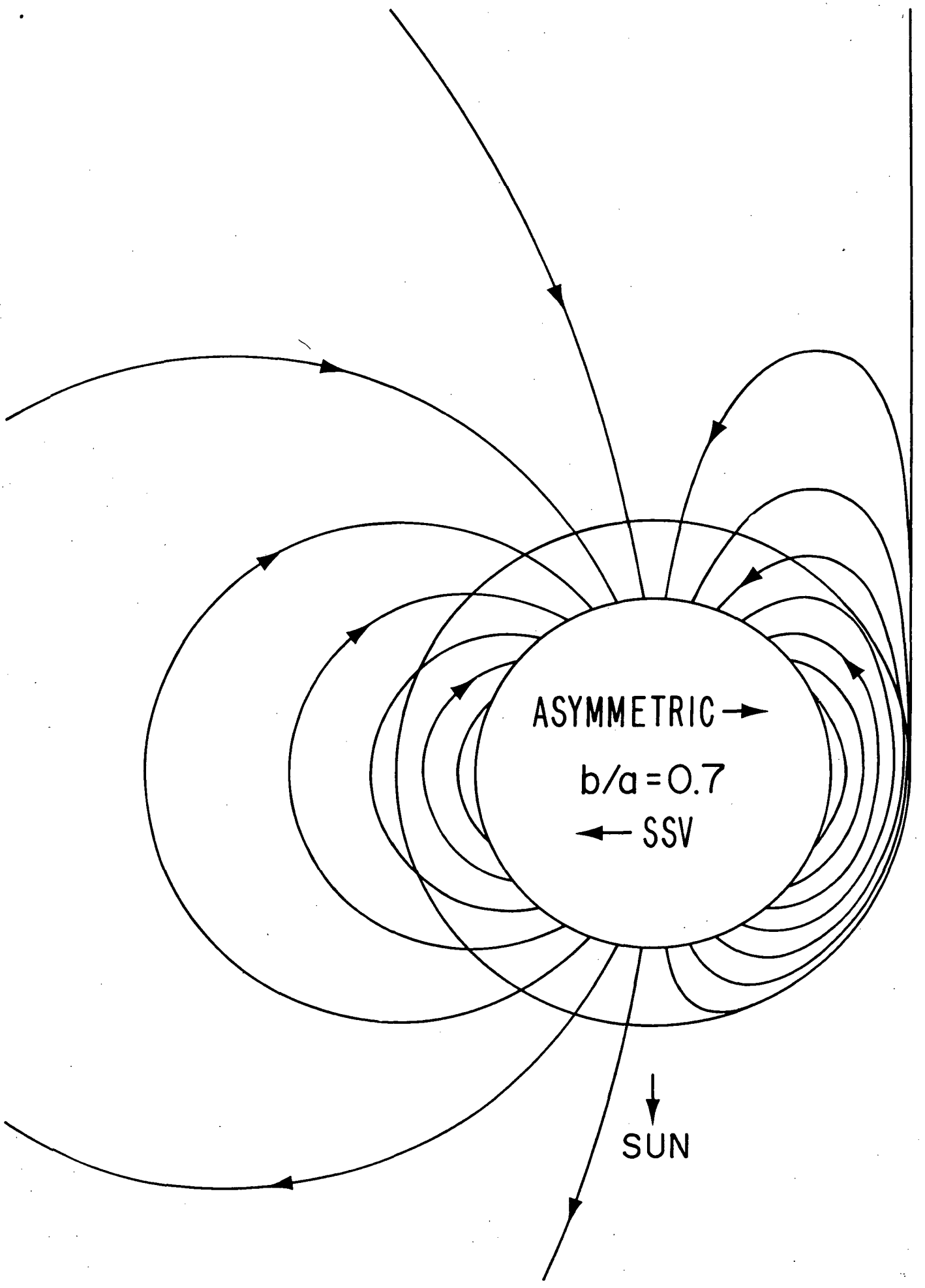
ASYMMETRIC →
b/a = 0.7
← SSV
SUN

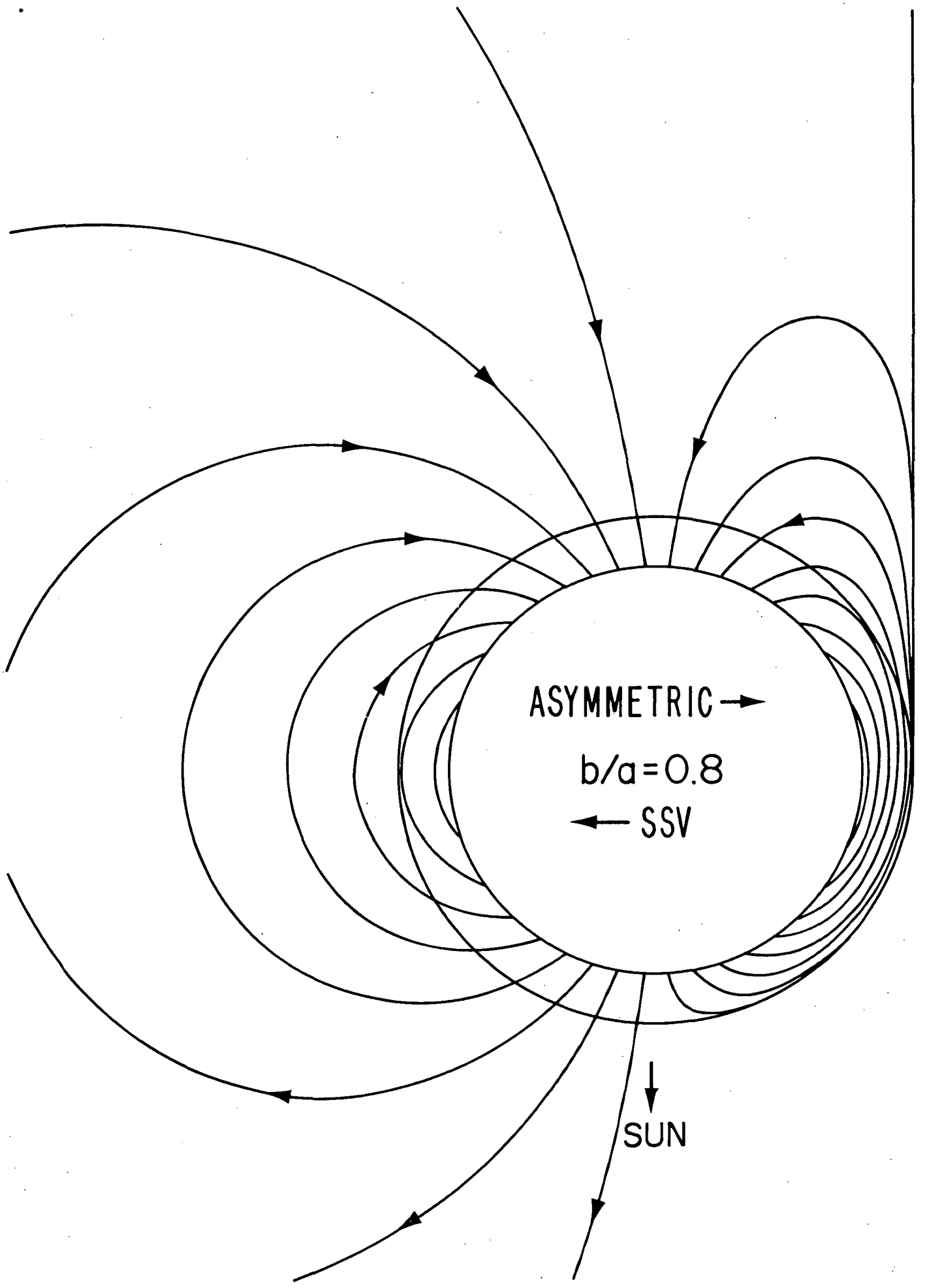
ASYMMETRIC →
b/a=0.8
← SSV
SUN

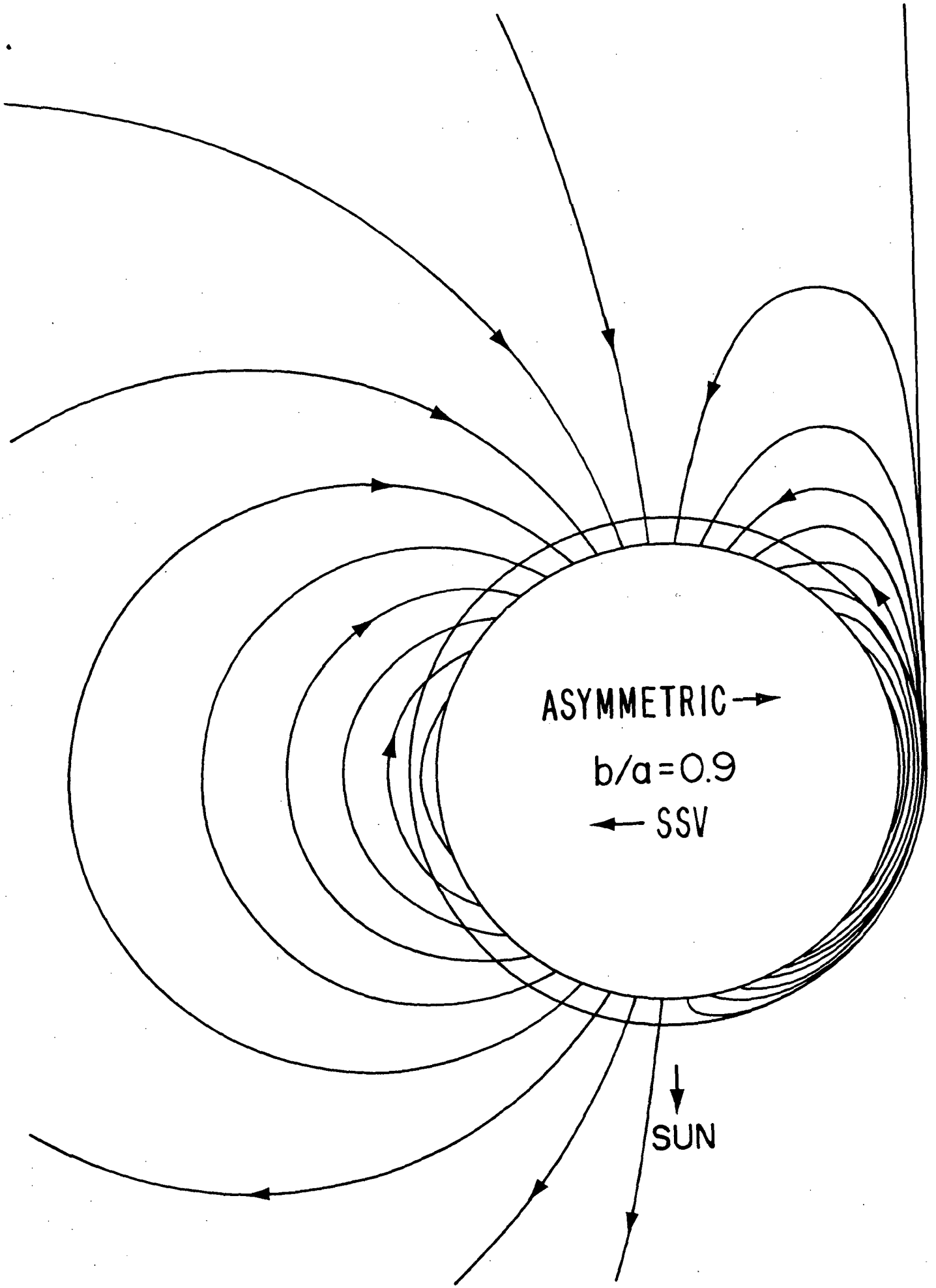
ASYMMETRIC →
b/a=0.9
← SSV
SUN

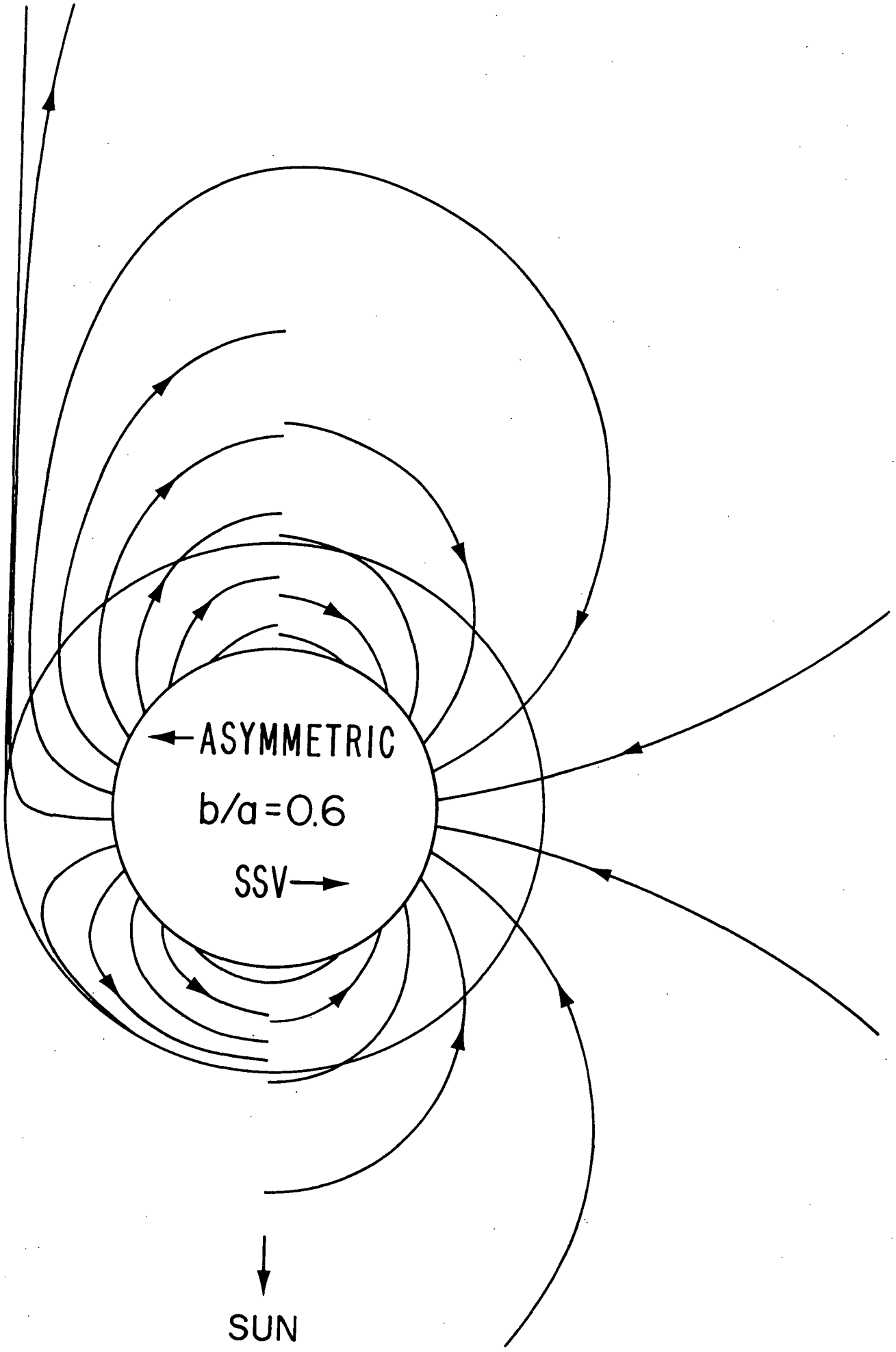
ASYMMETRIC
b/a=0.6
SSV
SUN

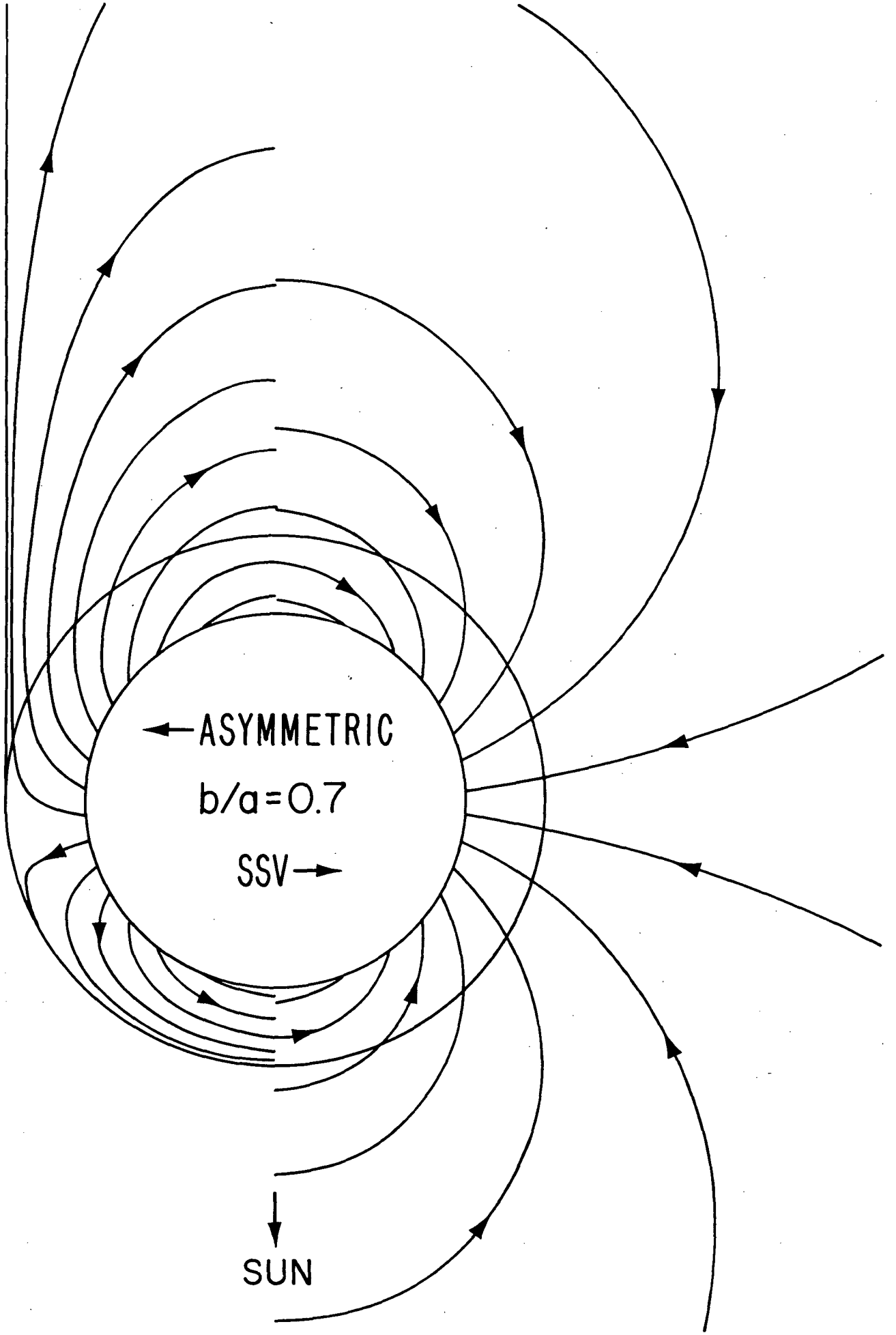
ASYMMETRIC
b/a=0.7
SSV
SUN

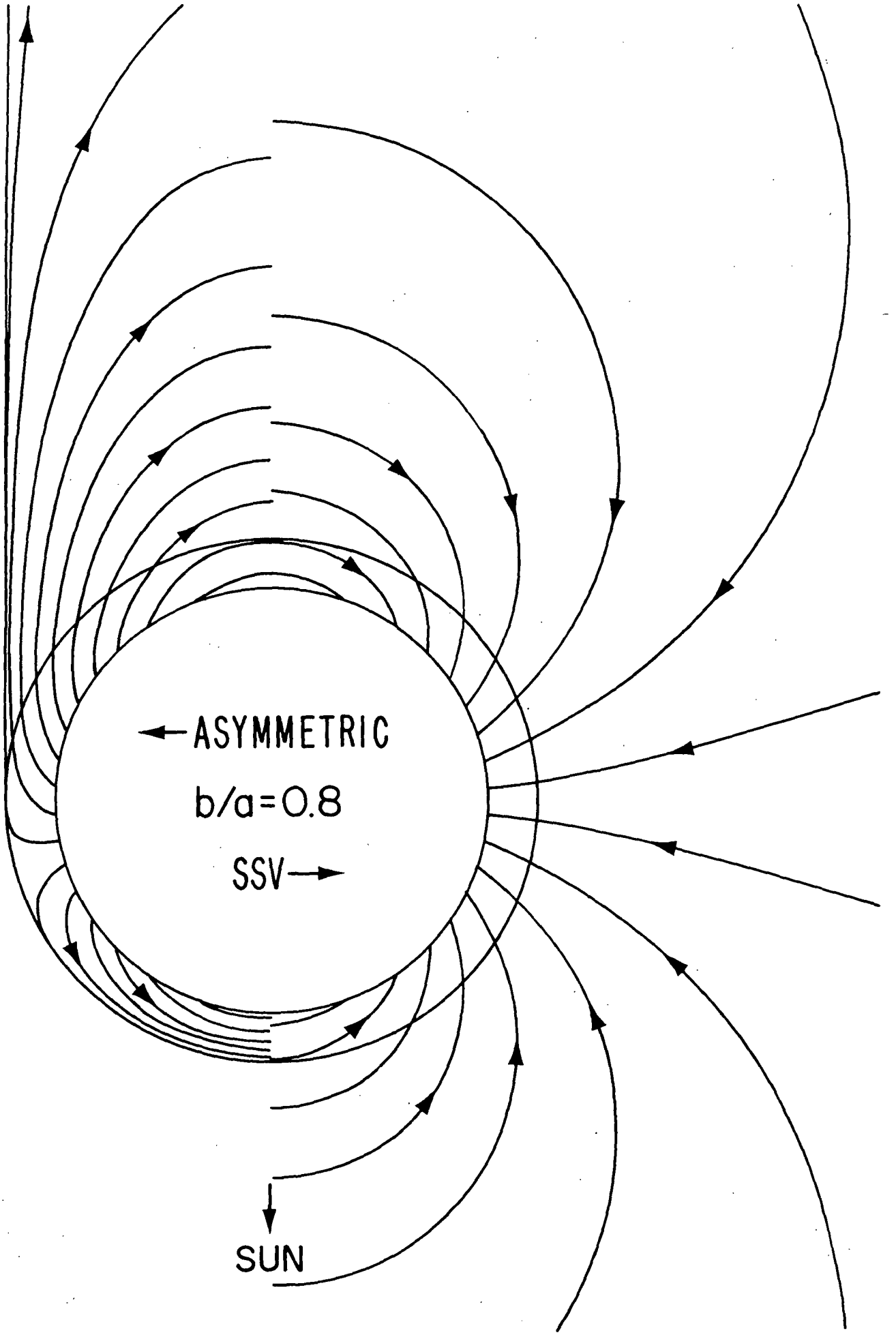
ASYMMETRIC
b/a=0.8
SSV
SUN

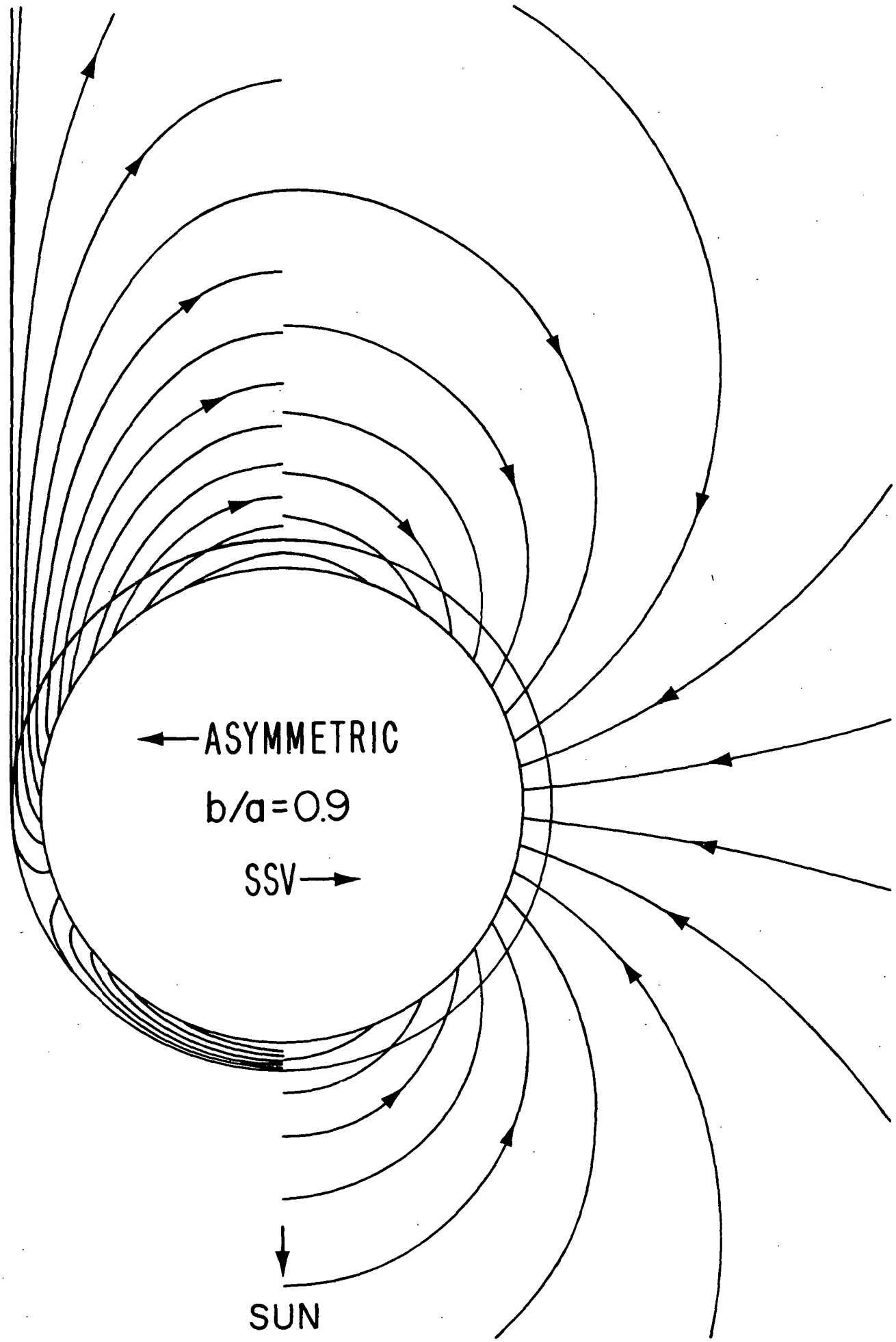
ASYMMETRIC
b/a=0.9
SSV
SUN